
The Combined Effects of Doxorubicin and a Novel Sulfonamide Derivative on Inducing Apoptosis in a Breast Cancer Cell Line (MCF-7)

Shabnam Pedarpour , Sevda Zarei , Zeinab Mahmoodi , [Hossein Ghafouri](#) *

Posted Date: 21 February 2024

doi: 10.20944/preprints202402.1233.v1

Keywords: Apoptosis; Breast cancer; Drug synergism; Doxorubicin; Sulfonamide



Preprints.org is a free multidiscipline platform providing preprint service that is dedicated to making early versions of research outputs permanently available and citable. Preprints posted at Preprints.org appear in Web of Science, Crossref, Google Scholar, Scilit, Europe PMC.

Copyright: This is an open access article distributed under the Creative Commons Attribution License which permits unrestricted use, distribution, and reproduction in any medium, provided the original work is properly cited.

Article

The Combined Effects of Doxorubicin and a Novel Sulfonamide Derivative on Inducing Apoptosis in a Breast Cancer Cell Line (MCF-7)

Shabnam Pedarpour ¹, Sevda Zarei ¹, Zeinab Mahmoodi ¹ and Hossein Ghafouri ^{2,*}

¹ Department of Biology, Faculty of Science, University of Guilan, Rasht, Iran

² Department of Marine Sciences, the Caspian Sea Basin Research Center, University of Guilan, Rasht, Iran

* Correspondence: H.ghafoori@guilan.ac.ir; Tel.: +981333333647

Abstract: Chemical combinations are believed to reduce drug toxicity, delay cancer cell growth, and achieve enhanced efficacy compared with single active drugs. This research investigated the synergistic effect of DOX and Zm-093, a new sulfonamide derivative, on improving the potential for inducing apoptosis in breast cancer (BC) cell lines. First, the Zm-093 compound was synthesized and its structure was confirmed by FT-IR and NMR. Then, the IC₅₀ values for DOX and Zm-093 were calculated to be 1.21 and 51.24 μM, respectively. To investigate the synergistic effect, CompuSyn software was utilized to calculate the combination index (CI). Different methods, including western blotting, flow cytometry, and TUNEL, were used to evaluate the potential synergistic effects of these compounds on inducing apoptosis in MCF-7 cells. Combining the indexes obtained at all concentrations revealed synergistic results. The proapoptotic proteins Bax, tBid, and caspase-3, however, increased 2.4, 3.3, and 5.7 times more than those in the control group. Flow cytometry analysis and the TUNEL method in cells treated with DOX and Zm-093 showed that apoptosis was significantly higher than in other groups. The results confirmed the synergistic effect of DOX and ZM-093 on apoptotic factors expression in MCF-7 cells.

Keywords: apoptosis; breast cancer; drug synergism; Doxorubicin; sulfonamide

1. Introduction

BC is the most prevalent cancer among women, with approximately 2.2 million cases diagnosed in 2020. Currently, BC is the leading cause of tumor-related mortality worldwide [1,2]. BC is diagnosed using pathological examinations and hormonal and molecular analyses of tissue samples [2]. BC management is multifaceted. Various therapeutic approaches are employed in treating BC, considering factors such as the specific cancer type, stage of disease progression, and overall health status of the patient. Therapeutic modalities encompassing surgery, radiotherapy, hormone therapy, chemotherapy, molecular therapies, and photodynamic therapy have been identified as notable interventions in the field [3]. Combination therapy in cancer treatment holds potential benefits for patients, as it can enhance response rates and mitigate adverse effects associated with cancer therapies [4].

A promising aim for cancer treatment is the induction of apoptosis [5–7], a natural mechanism for death in cells. Apoptosis is an active process that regulates and maintains individual cells and tissues [8,9]. There are at least two general signaling pathways that activate apoptosis: the intrinsic (mitochondrial) and extrinsic (death receptor) pathways [10]. Research shows that apoptosis is actuated by intracellular and extracellular signals. Intracellular signals include DNA damage, deprivation of growth factors, and deprivation of cytokines. Extracellular signals include death-inducing signals released from cytotoxic cells of the immune system due to damaged or infected cells. The executioner caspases converge the pathways. In cancerous cells, apoptosis pathways are generally inhibited through mechanisms involving the decreased expression of proapoptotic proteins

(for example, Bax and tBid) and the overexpression of antiapoptotic proteins (for example, Bcl-2) [11,12].

Cancer therapy relies heavily on anticancer compounds, which have been deemed vital to the fight against cancer. Currently, the U.S. Food and Drug Administration (FDA) has granted approval for more than one hundred medications specifically designed for this purpose [13]. Nevertheless, drug resistance and adverse off-target outcomes influence the efficacy of cancer therapy [14]. Medicinal chemists are tasked with designing novel anticancer drugs that exhibit elevated specificity and potency while effectively mitigating off-target effects and drug resistance [15].

Compounds containing a sulfonamide moiety are typically synthesized by reacting R-sulfonyl chloride with primary or secondary amines in a basic environment [16]. Recently, research has focused on molecules that incorporate sulfonamide fragments. This heightened interest can be attributed to the several possible uses of these compounds in various fields, such as coordination chemistry [17], medicinal chemistry, and analytical chemistry [18]. In contrast, sulfonamide compounds are recognized for their intrinsic pharmacological characteristics, including antibacterial [18,19], anti-inflammatory, antiviral, antiproliferative, and angiogenic properties [20].

Doxorubicin (DOX) is a chemotherapeutic agent used to treat several malignancies. The mechanism of action involves DNA interactions, namely, intercalation and inhibition of macromolecular formation, ultimately resulting in cellular death. However, the therapeutic efficacy of DOX is impeded by notable adverse reactions and drug resistance development [21]. In addition to alopecia, myelosuppression, emesis, dermatitis, and other minor adverse effects, DOX has the potential to cause severe hypersensitivity reactions, cardiotoxicity, radiation recall, therapy-related leukemia, and palmar-plantar erythrodysesthesia [22]. Multiple studies have demonstrated that chemical coadministration of different pharmacological agents may successfully reduce the adverse effects of DOX while concurrently augmenting its pharmacological responsiveness [23].

DOX exerts its effect mainly through changes in and interference with DNA, and according to previous studies, a new sulfonamide derivative (Zm-093) causes cell death by changing the expression of factors in the internal pathway of apoptosis [24]. In this study, we investigated the anticancer and antigrowth effects of DOX and Zm-093, as well as the potential synergistic effects of these compounds on inducing apoptosis via different methods, including western blotting, flow cytometry, and TUNEL staining, on MCF-7 cells (a human BC cell line).

2. Results

2.1. Antiproliferative activity against the MCF-7 cell line

MCF-7 cells were treated for 24 hours with DOX and the synthetic compound Zm-093 to determine their cytotoxic effects (Figure 1). The survival rate of cancer cells was significantly lower in the DOX and Zm-093 treatment groups than in the control group. Cancer cell proliferation was inhibited by these compounds in a dose-dependent manner ($P < 0.0001$). The IC_{50} values for DOX and Zm-093 were calculated to be 1.21 and 51.24 μ M, respectively (Figure 1a and 1b).

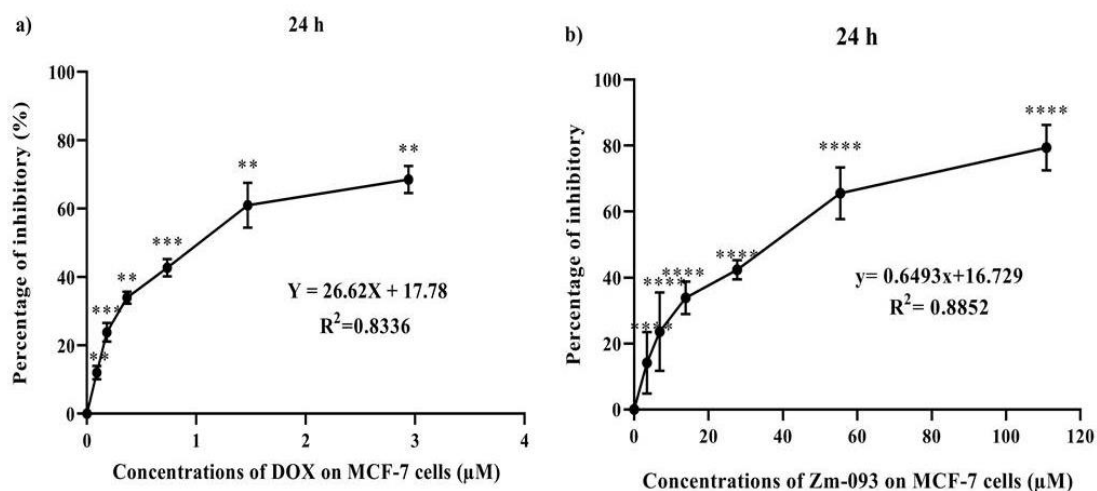
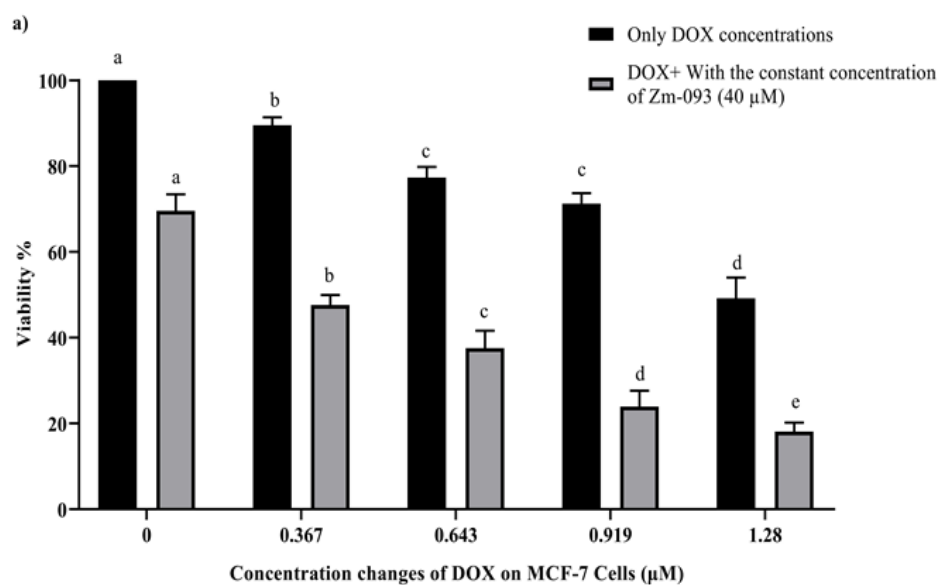


Figure 1. Determination of DOX and Zm-093 IC_{50} in MCF-7 cells (mean \pm SD). **a)** The IC_{50} of DOX was 1.21 μ M. The growth inhibition rate increased with increasing dose. **b)** The IC_{50} of Zm-093 was 51.24 μ M. A dose-dependent increase in growth inhibition was observed. The process for each treatment group was repeated three times. The letters within each column indicate significantly different groups based on a one-sample t test ($P < 0.0001$).

2.2. The synergistic effects of DOX and Zm-093 on MCF-7 cell viability

To investigate the synergistic effect of DOX and the Zm-093 compound on the viability of MCF-7 cells, the cells were treated with different concentrations of DOX and Zm-093 alone and in combination with each other at a constant concentration of 0.36 μ M (this concentration is approximately 30% of the IC_{50} that was studied) for DOX and 40 μ M for Zm-093 for 24 h (Figure 2 and Figure 3). The survival rate decreased significantly with increasing dose in both combinations ($P < 0.0001$). In addition, DOX and Zm-093 had synergistic effects at fixed concentrations, and in the combined treatment, cell viability was significantly reduced ($P < 0.0001$; Figure 2a and Figure 3a).

The optical density (OD) was subsequently read by an Eliza reader spectrophotometer for DOX and the Zm-093 compound alone and in combination (Table 1 and Table 2). Next, to probe the synergistic effect, the combined index or CI of these compounds at various concentrations were evaluated via CompuSyn software (Figure 2b and Figure 3b). According to the results obtained with this software, all the combination Fa (fraction affected) values were less than 1, confirming the synergistic effect between DOX and Zm-093.



b) **Combination Index Plot**

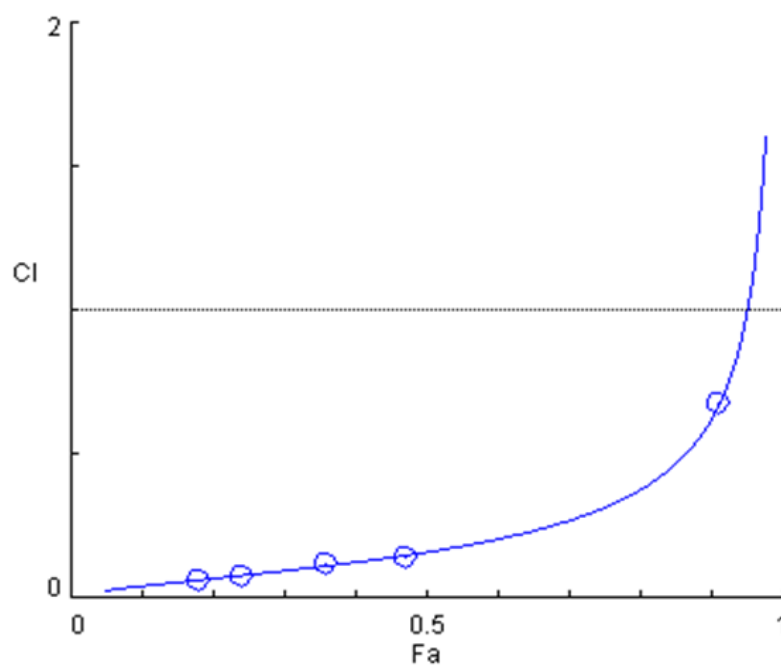
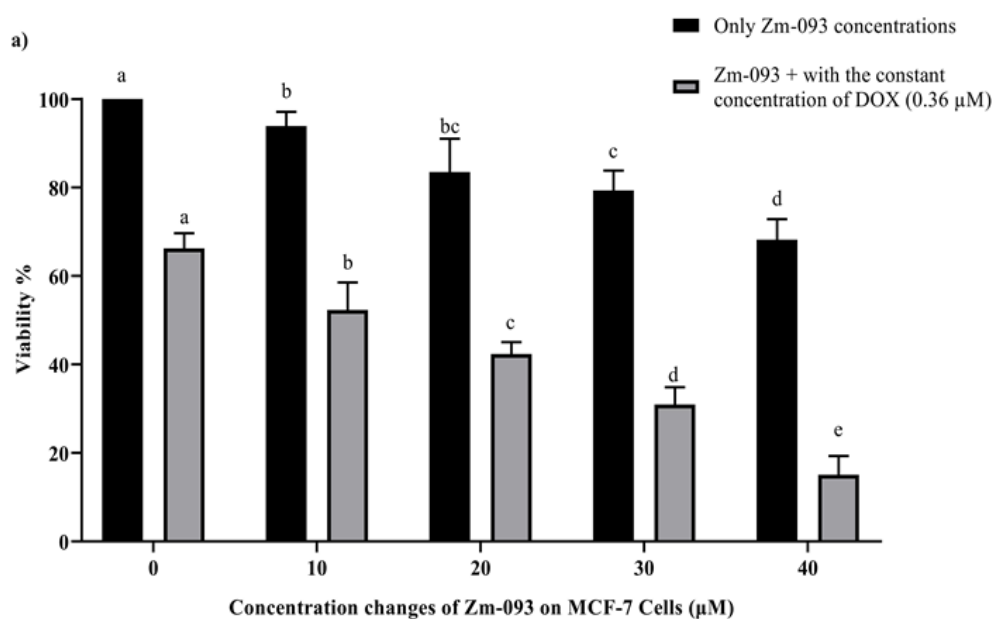


Figure 2. Survival and combination indexes (CI) at variable and constant concentrations of DOX and Zm-093 (mean \pm SD). a) Viability (%), b) CI plot. A constant concentration of 40 μ M was used for Zm-093, and 0, 0.367, 0.643, 0.919, and 1.28 μ M were utilized for DOX. Growth inhibition increased in a dose-dependent manner. The value of CI < 1 was. There were three replicates for each treatment group. Within each column, different letters indicate significantly different groups according to Duncan's test (a, b, c, and...; $P < 0.0001$).



b) Combination Index Plot

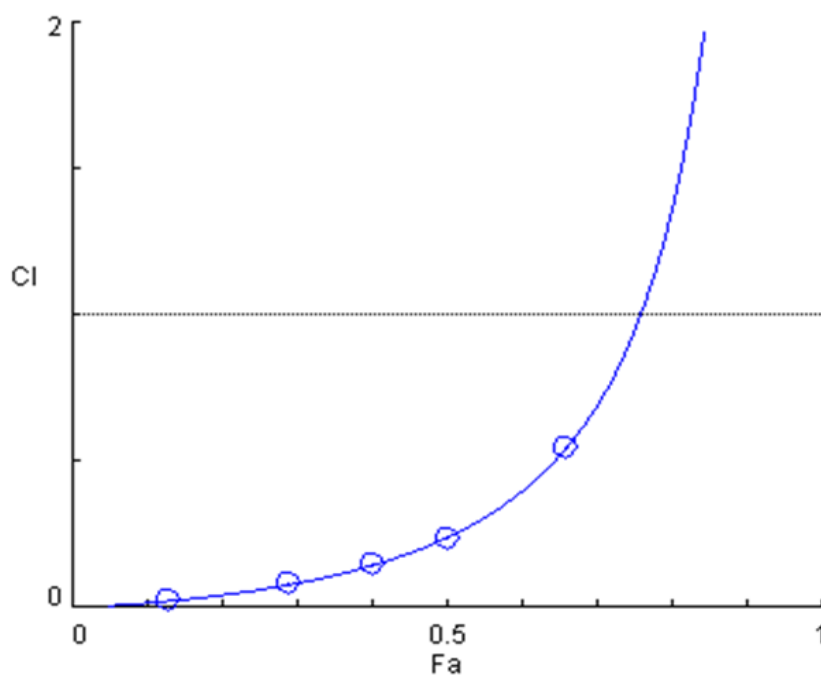


Figure 3. Survival and combination indexes (CI) at variable and constant concentrations of Zm-093 and DOX (mean ± SD). a) Viability (%), b) CI plot. A constant concentration of 0.36 μM was used for DOX, and 0, 10, 20, 30, and 40 μM were utilized for Zm-093. There was a dose-dependent increase in growth inhibition. The value of CI < 1 was. For each group, the treatment was repeated three times. Within each column, different letters indicate significantly different groups according to Duncan's test (a, b, c, and...; $P < 0.0001$).

Table 1. OD values for MCF-7 cells treated with different concentrations of DOX and Zm-093 alone for 24 h.

| Groups | Zm-093 (μM) | DOX (μM) | Fraction affected (Fa) | Combination index (CI) |
|--------|-------------|----------|------------------------|------------------------|
| 1 | 40 | 0 | 0.69 | 0 |
| 2 | 40 | 0.367 | 0.47 | 0.14051 |
| 3 | 40 | 0.643 | 0.36 | 0.12282 |
| 4 | 40 | 0.919 | 0.24 | 0.07672 |
| 5 | 40 | 1.28 | 0.18 | 0.06369 |

Table 2. The OD values for MCF-7 cells treated with different concentrations of Zm-093 and DOX alone after 24 h.

| Groups | DOX (μM) | Zm-093 (μM) | Fraction affected (Fa) | Combination index (CI) |
|--------|----------|-------------|------------------------|------------------------|
| 1 | 0.36 | 0 | 0.66 | 0 |
| 2 | 0.36 | 10 | 0.5 | 0.23781 |
| 3 | 0.36 | 20 | 0.4 | 0.14568 |
| 4 | 0.36 | 30 | 0.29 | 0.07974 |
| 5 | 0.36 | 40 | 0.13 | 0.02215 |

2.3. Measurement of apoptotic and antiapoptotic protein expression by western blotting

The apoptotic effects of DOX (0.36 μM) and Zm-093 (14.5 μM) alone or in combination (0.36 μM DOX + Zm-093 at 14.5 μM) on MCF-7 cells were examined. In total, the study included four groups: a control group (no treatment), a DOX group, a Zm-093 group, and a DOX+Zm-093 group. The levels of proapoptotic (tBid, Bax, and caspase-3) and antiapoptotic (Bcl-2) proteins were analyzed via western blotting (Figure 4). Original photos of the western blot gel are available in Supplementary Figure 3.

2.3.1. tBid

The DOX (2.56-fold) and Zm-093 (2.43-fold) groups exhibited similar changes in protein tBid relative expression, but there was a significant increase compared to the control group ($P < 0.0001$). Moreover, DOX+Zm-093 (3.39-fold) showed the highest level of tBid protein expression ($P < 0.0001$; Figure 4a and 4b).

2.3.2. Bax

There was a considerable increase in Bax protein expression compared to that in the control group, similar to the changes in the protein tBid in the DOX (2.16-fold) and Zm-093 (2.25-fold) groups. DOX+Zm-093 also increased Bax protein expression (2.53-fold, $P < 0.0001$; Figure 4c and 4d).

2.3.3. Caspase-3

When MCF-7 cells were treated with DOX or Zm-093, caspase-3 was in a procaspase-3 or cleaved caspase-3 state, respectively. Compared to those in the control group, all the treatment groups had lower pro-caspase-3 levels. Compared to those in the control group, the changes in expression increased after caspase-3 was cleaved. Therefore, we observed the highest expression of caspase-3 in the DOX+Zm-093 group (5.73-fold, $P < 0.0001$; Figure 4e and 4f).

2.3.4. Bcl-2

There was a difference in the Bcl-2 protein levels in the treated MCF-7 cells in the presence of the test compounds. In the Zm-093 group (1.03-fold), the changes in the Bcl-2 protein were similar to those in the control group. Compared to those in the control group, the DOX group produced less

Bcl-2 protein (0.741-fold). The lowest level of Bcl-2 expression was also found in the DOX+Zm-093 group (0.562-fold, $P < 0.0001$; Figure 4g and 4h).

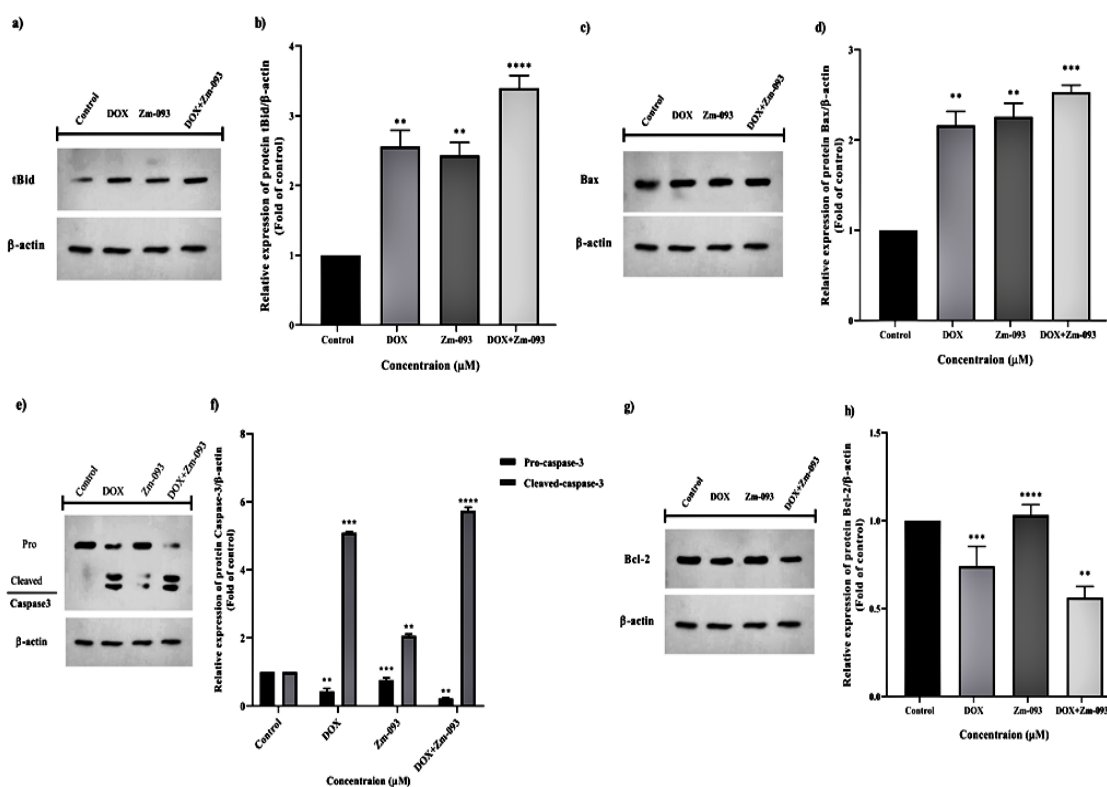


Figure 4. The relative expression of proapoptotic and antiapoptotic proteins was determined via western blotting. a) and b) tBid, c) and d) Bax, e) and f) caspase-3, g) and h) Bcl-2. The cells were divided into 4 groups: 1. control cells without treatment and 2. DOX (0.36 μM), 3. Zm-093 (14.5 μM), and 4. DOX+Zm-093 (0.36+14.5 μM). The protein levels are shown as the fold change relative to the control values (mean \pm SD), and each parameter was measured three times. Within each column, different letters indicate significantly different groups according to a one-sample t test ($P < 0.0001$).

2.4. Apoptotic/necrotic ratios in MCF-7 cells

As shown in Figure 5, there were three groups according to flow cytometry: a control group (no treatment), a DOX group (0.36 μM), and a DOX+Zm-093 group (0.36 + 22 μM). The incidence of early apoptosis differed among the three treatment groups. Compared with control cells (4.28%) or DOX-treated cells (5.21%), cells treated with DOX+Zm-093 (13.2%) exhibited increased primary apoptosis. In addition, the DOX and DOX+Zm-093 groups exhibited greater rates of late apoptosis (4.90% and 3.96%, respectively) than did the control group (1.88%). In contrast, there was no significant difference in necrosis between the treated and control groups.

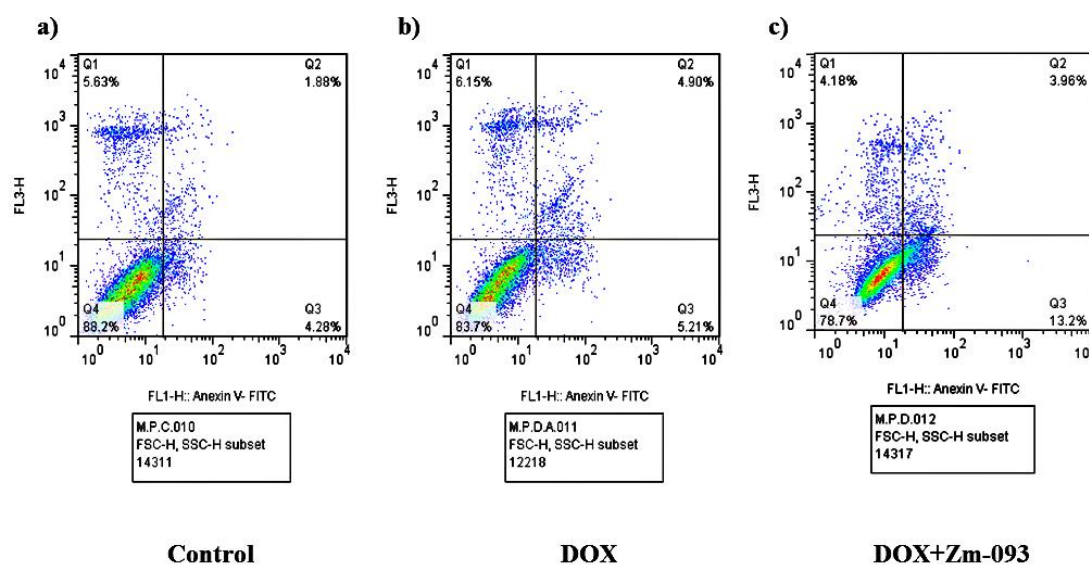


Figure 5. Analysis of apoptosis by flow cytometry with Annexin V/PI staining in MCF-7 cells. Flow cytometry was performed on three groups: a control group (no treatment), a DOX group (0.36 μ M), and a DOX+Zm-093 group (0.36 + 22 μ M). The incidence of early apoptosis differed among the three treatment groups.

2.5. TUNEL assay of treated MCF-7 cells

Apoptotic cells exhibit typical nuclear condensation as a morphological sign. As DNA strands are cleaved or nicked by nucleases, many 3'-hydroxyl ends are exposed. TUNEL assays were performed to detect cells that exhibited massive DNA fragmentation, a sign of late apoptosis (Figure 6). The study included four groups: a control group (no treatment), a DOX group (0.36 μ M), a Zm-093 group (14.5 μ M), and a DOX + Zm-093 group (0.36 + 14.5 μ M). The amount of fragmented DNA in MCF-7 cells treated with the simultaneous combination of two compounds (DOX + Zm-093) increased compared to that in the control group and cells treated with each compound alone (DOX or Zm-093), indicating that the combination of the two compounds induces more apoptosis ($P < 0.0001$).

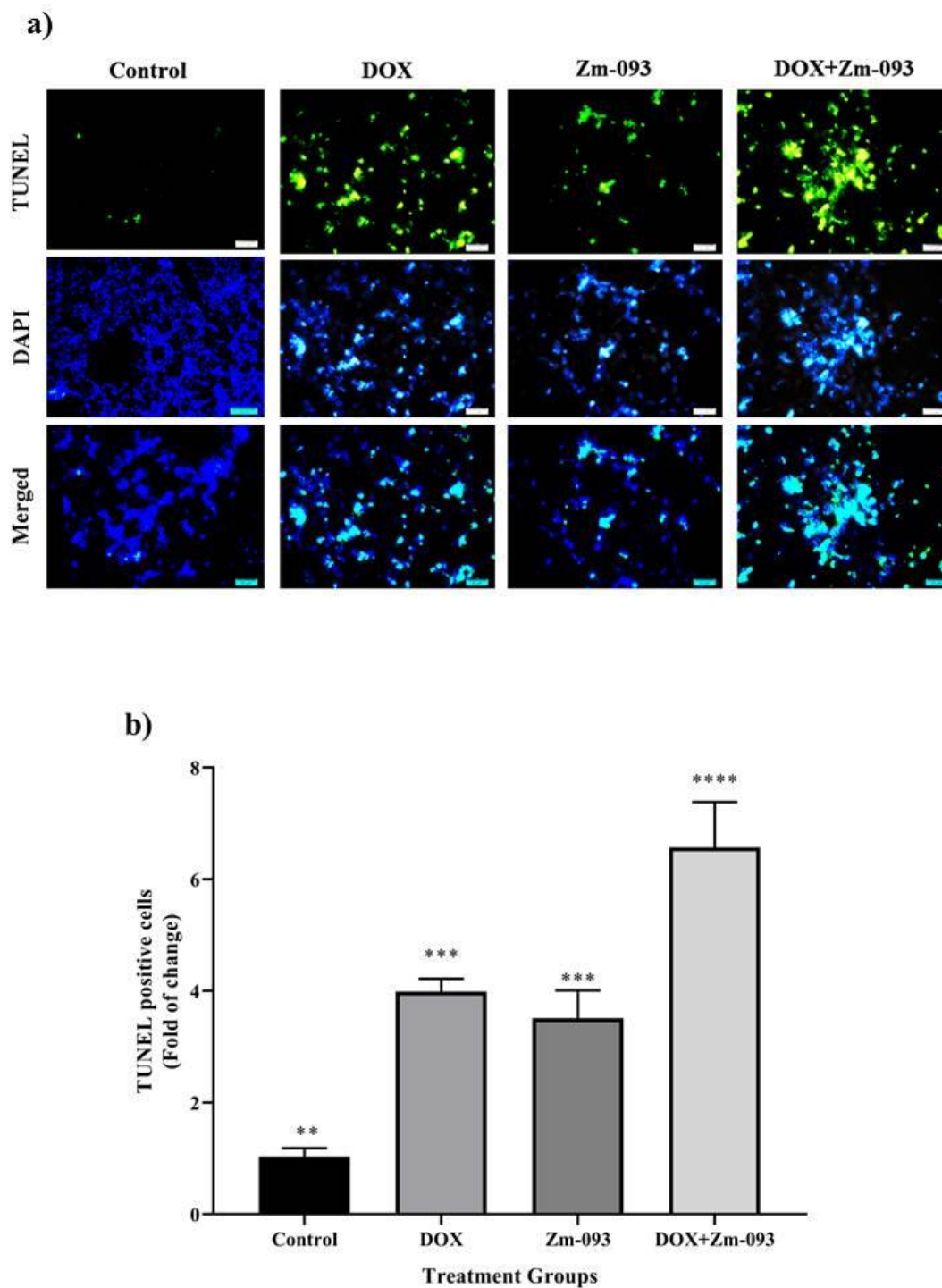


Figure 6. Assessment of the apoptosis rate in MCF-7 cells using the TUNEL test at 400x magnification. **a)** 4 groups were considered: 1. control cells without treatment, 2. DOX (0.36 μ M), 3. Zm-093 (14.5 μ M), and 4. DOX+Zm-093 (0.36 + 14.5 μ M). Combining two compounds (DOX + Zm-093) increased fragmented DNA levels in MCF-7 cells. **b)** A quantitative analysis of apoptotic nuclei was performed (mean \pm SD). The letters within each column indicate significantly different groups based on a one-sample t test ($P < 0.0001$).

3. Discussion

The goal of clinical treatment is to suppress and eliminate tumors, and chemotherapy is crucial for achieving this goal. The inherent limitations of single chemotherapy treatments lead to the use of combinational medications in clinical settings [33]. Combining the right medicines is essential. DOX induces cellular apoptosis by inhibiting DNA replication and suppressing protein synthesis, making it an effective treatment option for a wide range of malignant malignancies. In general, tumors respond to DOX when it is administered alone or in combination with other anticancer medicines. However, the use of this substance is limited by the occurrence of dose-limiting toxicities and increased drug resistance [34,35]. Consequently, new combinations of drugs that can enhance or sustain effectiveness while mitigating toxicity and retarding the emergence of drug resistance must be explored [36]. In addition to their anticancer properties, sulfonamide-derived compounds exhibit a variety of biological actions. These compounds are heterocycles that can form hydrogen bonds. As a result, these peptides are more soluble and more likely to interact with biomolecular targets due to this property. The potential of sulfonamide derivatives as cancer medicines has been extensively studied [37,38].

The purpose of this study was to determine whether DOX and a new sulfonamide derivative (Zm-093) can interact synergistically to induce apoptosis in MCF-7 cells. The IC_{50} values for DOX and Zm-093 were calculated to be 1.21 and 51.24 μM , respectively. According to the obtained IC_{50} values, first, DOX was used at a constant concentration of 0.36 μM , and Zm-093 was used at concentrations of 0, 10, 20, 30, and 40 μM ; second, a constant concentration of 40 μM was used for Zm-093, and at concentrations of 0, 0.367, 0.643, 0.919, and 1.28 μM , was used for DOX. The Chou-Talalay approach was employed in this investigation to quantify the synergistic effects of DOX and Zm-093 utilizing the Compusyn program. The CI was plotted on the y-axis as a function of the effect level (Fa) on the x-axis to assess the potential synergistic effect between DOX and Zm-093 on MCF-7 cells. According to the Chou-Talalay technique, the CI determines the synergistic effect of two substances. A CI value less than 1 signifies a synergistic effect, a CI value equal to 1 indicates an additive effect, and a CI value greater than 1 suggests a possibly antagonistic impact [39]. When DOX and Zm-093 were combined, cell survival decreased, and cell death increased in MCF-7 cells at all concentrations. A synergistic effect was observed when Zm-093 was combined with DOX at concentrations ranging from 10 to 20 μM , while the fixed DOX concentration was maintained at 0.36 μM . The same effect was observed at fixed Zm-093 (40 μM) concentrations and variable DOX concentrations. A calculated CI value of less than 1 demonstrated this. According to previous studies, the combination of the ruthenium(II) complex and DOX has significant synergistic effects on inhibiting MCF-7 cell proliferation [40]. Synergism and antagonism are quantitatively defined by the CI theorem and the median-effect equation (MEE) in the mass-action law. These approaches provide straightforward, efficient, and cost-effective means of assessing the combined effects of medications, allowing them to be widely used worldwide [41].

The combined effects of several factors, including Bcl-2, Bax, tBid, and caspase-3, on the expression of proteins involved in the intrinsic apoptosis pathway were evaluated by Western blotting. Both the intrinsic and extrinsic pathways can trigger apoptosis. Proapoptotic Bcl-2 family members, such as Bax and Bak, initiate this pathway. As these entities oligomerize and integrate within the mitochondrial outer membrane, they form holes and initiate mitochondrial outer membrane permeabilization (MOMP). Therefore, cytochrome C is discharged from the mitochondria and translocated from the intermembrane gap to the cytosol. The presence of cytochrome C in the cytosol triggers the oligomerization of peptidase-activating factor 1 (Apac-1). As a result of this event, caspase-9 is recruited to and activated within an apoptotic complex. Apoptosis or programmed cell death is caused by caspase-9, an initiator caspase. In response to caspase-9 activation, the downstream effectors caspase-3 and caspase-7 are cleaved and triggered. The cleavage of essential regulatory and structural proteins causes cell death [41,42]. By administering DOX and Zm-093 simultaneously, Bcl-2 expression was reduced compared to that in the DOX and Zm-093 alone group or the control group. Afterward, we focused on the proapoptotic property of Bax, which was isolated from cells treated with DOX and Zm-093. The combination of these two drugs significantly enhanced

the expression of this protein compared to that in the control group. In addition, since the Bax/Bcl-2 relationship regulates cytochrome C release and because its impact on cell death acceleration is crucial, we examined the Bax/Bcl-2 ratio in our study. Similarly, compared with those of the control, the Bax/Bcl-2 ratio increased 2.91-fold in response to treatment with DOX alone, 2.18-fold in response to treatment with Zm-093 alone, and 4.5-fold in response to the simultaneous combination of these two medications. The modulation of the Bax/Bcl-2 ratio was demonstrated by concurrently combining the two compounds. The combination of two chemicals also had synergistic effects on tBid expression more strongly than the individual chemical treatments did, suggesting that caspase 8 was activated more strongly due to external apoptosis [7]. The DOX, Zm-093, and combined treatment groups (DOX+Zm-093) had higher caspase-3 levels than did the control group (5.08-fold, 2.06-fold, and 5.73-fold, respectively). In addition, 2.78-fold more MCF-7 cells treated with DOX and Zm-093 coexpressed active caspase-3 than cells treated with Zm-093 alone. In contrast, the expression of the partial caspase-3 protein was increased in the DOX-treated group compared to the DOX alone group.

In a study conducted by Shi et al. investigating the synergistic impact of DOX and glycyrrhetic acid on MCF-7 cells, it was observed that the concurrent administration of these two compounds resulted in a significantly enhanced and more productive upregulation of the Bax/Bcl-2 ratio, as well as the active caspase-3/inactive caspase-3 ratio, in comparison to individual treatments [44]. In the next study, researchers examined the potential synergistic impact of combining DOX with a mushroom extract (*Herichium*) on hepatic cells. The study results indicate that combined treatments elicit a more pronounced effect on upregulating Bax and caspase-3 while concurrently downregulating Bcl-2 expression than individual treatments alone [45]. Moreover, TUNEL staining revealed that the combined administration of phenethyl isothiocyanate and paclitaxel resulted in a significant increase in apoptosis in MCF-7 cells in comparison to the individual treatments of these agents. Specifically, the combination treatment led to a 3.4-fold increase in apoptosis compared to phenethyl isothiocyanate alone and a 2.8-fold increase compared to paclitaxel only. These findings provide evidence for the enhanced apoptotic effect of the drug combination on MCF-7 cells [46]. In line with the findings of previous studies, the flow cytometry results demonstrated that the coadministration of DOX and Zm-093 had a more significant apoptotic impact on MCF-7 cells, characterized by increased levels of primary and late apoptosis, than the individual administration of both anticancer drugs. TUNEL staining further demonstrated that the apoptosis rates of cells treated with DOX and Zm-093 alone and in combination were increased by 3.8, 3.4, and 6.3 times, respectively. Additionally, the percentage of apoptotic cells was 1.6 and 1.8 fold greater in the group receiving the combined treatment of DOX and Zm-093 than in the groups receiving monotherapy with DOX and Zm-093, respectively. These findings indicated a significant increase in the number of cells undergoing apoptosis, highlighting the remarkable apoptotic effect observed in cancer cells treated with the combination of these treatments.

4. Materials and methods

4.1. Synthesis of azo compounds based on 2-amino-5-mercapto-1,3,4-thiadiazole (Zm-093)

Zm-093 (an azo dye based on sulfamethoxazole) was prepared through common diazotization-coupling reactions in high yield. The diazonium salt was prepared from an equal mixture of sulfonamide derivative (2 mmol of sulfamethoxazole, 4 mL of acetonitrile, and a few drops of acetic acid), and HNO₂ (NaNO₂ and HCl) was prepared. Then, β-naphthol was used to ensure the synthesis of the diazonium salt. The diazonium salt from the previous step was added dropwise to the mixture containing the pair reagent (N-phenyl-2,2-iminodiethanol in ethanol). The resulting solution was stirred vigorously for 2 h at 0-4°C. After that, the pH of the solution was maintained within the physiological pH range by the addition of NaOH. Thin-layer chromatography (TLC) was used to evaluate the progress of the reaction. The crude product was filtered and washed with water three times. Zm-093 was isolated by recrystallization. NMR and FT-IR (Supplementary Figure 1 and 2) spectroscopy confirmed the structure of the obtained azo dye [25].

4.2. Cell culture

The MCF-7 cell line, derived from human BC, was purchased from the Pasteur Institute of Iran. All cell culture materials were obtained from Bioidea in Iran. The cells were cultivated in culture medium supplemented with L-glutamine, 90% RPMI 1640, 10% fetal bovine serum (FBS), and 100 U/mL streptomycin/penicillin (1%) in T-25 cm² flasks at 37°C, 5% CO₂, and 95% humidity. After approximately 24 h, the culture medium inside the flask was replaced with fresh medium. Microscopic examination of the cells was conducted daily to check for contamination and growth. After 3-5 days, the cells reached 80-90% confluence. The cells were then treated with trypsin-EDTA (0.25%). To do this, the culture medium was removed from the flask, and the cells adhering to the bottom of the flask were washed twice with phosphate-buffered saline (PBS). Trypsin-EDTA was added to the cells, which were dispersed throughout the flask. After 3 min, the cells were centrifuged at 3000 rpm for 5 min. The supernatant was discarded, and the cell pellet was transferred to a flask for further treatment [12,26].

4.3. Calculation of the IC₅₀ values for DOX and Zm-093

MCF7 cells (5×10^5 cells/mL) were counted and transferred to 96-well plates. The cells were then incubated at 37°C, 5% CO₂, and 95% humidity and cultured in medium supplemented with 90% RPMI 1640, 10% FBS, and 100 U/mL streptomycin/penicillin (1%). After 24 h, the medium was replaced with RPMI 1640 containing 1% FBS. The cells were then treated with different concentrations of DOX (prepared from the Faculty of Pharmacy at the University of Tehran) at 0, 0.091, 0.183, 0.367, 0.735, 1.47, and 2.94 μM and with Zm-093 at 0, 3.46, 6.92, 13.85, 27.71, 55.43, and 110.87 μM for 24 h. The untreated group was considered the control group. Afterward, the viability of the cells was assessed via the 3-(4,5-dimethylthiazol-2-yl)-2,5-diphenyl-2H-tetrazolium bromide (MTT) assay. All procedures were performed under aseptic conditions. We repeated each concentration three times in each well, and the final volume was 200 μL.

Note: Initially, a wide range of ranges was selected; subsequently, in repeated trials, the optimal range was determined. The concentrations that caused the least toxicity to the cells were then chosen after the appropriate range was selected. The DOX and Zm-093 compounds were dissolved in 1% of the final volume in DMSO and ethanol, respectively. Next, culture medium was added to the mixture. The control was applied to the solvent. Previous studies revealed that 1% DMSO and ethanol have no toxic effects on cells.

MTT assays were used to measure metabolic activity in cells to evaluate viability, proliferation, and cytotoxicity [27]. To determine the IC₅₀ of DOX and Zm-093 and determine their optimal doses, we conducted an MTT experiment. As a result of enzymatically reducing the tetrazolium salt, the formazan form, which has a purple-blue color, can be quantified through spectrophotometry [12,26]. To perform the test, at the end of the treatment period, all the wells were emptied. Fresh medium without FBS (which constituted 90% of the final volume of the wells) was mixed with a solution of MTT (5 mg/mL; Sigma-Aldrich) in a volume of 10 μL (which constituted 10% of the final volume of the wells). The plates were then incubated for 3-4 h at 37°C, 5% CO₂, and 95% humidity. The final volume of each well was 100 μL, and the supernatant was removed. The formazan crystals that formed were solubilized in 100 μL of dimethyl sulfoxide (DMSO; Sigma-Aldrich) for 30 min. The absorbance at 570 nm was subsequently measured using a microplate reader (Bio-Rad Laboratories, CA, USA). The percentage of inhibitory effects was calculated using the following formula:

$$\text{Percentage of inhibitory} = \left[1 - \left(\frac{\text{OD (treatment)}}{\text{OD (control)}} \right) \right] \times 100\%$$

4.4. Synergistic effects of DOX and Zm-093

As described in section 2.3, the same number of cells were cultured under the abovementioned conditions. The synergistic effects of the DOX drug and the Zm-093 synthetic compound on MCF-7 cells were investigated. As a next step, the cells were treated with DOX (0, 0.367, 0.643, 0.919, and 1.28 μM) and Zm-093 (0, 10, 20, 30, and 40 μM) alone or in combination with constant concentrations of

0.36 and 40 μM for DOX and Zm-093, respectively (these concentrations were approximately 30% of the IC_{50} determined in section 2.3). After 24 h, the MTT test was performed under the same conditions as in section 2.3, and cell viability was calculated according to the following formula [26].

$$\text{Cell viability} = \left[\frac{\text{OD (treatment)}}{\text{OD (control)}} \right] \times 100\%$$

Combination indexes (CI) are quantitative measures used to assess the nature of pharmacological interactions, specifically synergistic, additive, or antagonistic interactions. Based on the equation below, CompuSyn software (version 1.0; Ting Chao Chou and Nick Martin, Paramus, NJ) was used to calculate the CI [28,29].

$$CI = \frac{(D)1}{(Dx)1} + \frac{(D)2}{(Dx)2} + \frac{(D)1 \times (D)2}{(Dx)1 \times (Dx)2}$$

In the CI formula, (Dx)1 and (Dx)2 represent the doses of DOX and Zm-093 in combination that were needed to achieve the same efficacy as that of DOX (D)1 and Zm-093 (D)2 when used alone.

A $CI > 1$ indicated an antagonistic interaction, and a $CI < 1$ indicated a synergistic interaction; a CI between 0.2 and 0.4 indicated a strong synergistic interaction, and a CI equal to 1 indicated an additive interaction.

4.5. Western blot analysis

Briefly, 5×10^5 MCF-7 cells/mL were seeded in 6-well plates and exposed to DOX (0.36 μM) and Zm-093 (14.5 μM) alone and in combination with each other (DOX + Zm-093: 0.36 + 14.5 μM) for 24 hours. Subsequently, the cells were subjected to lysis utilizing a lysis solution supplemented with 1% proteinase inhibitors, namely, phenylmethylsulfonyl fluoride (PMSF), to ensure proteolytic inhibition. Following lysis, the total protein content was extracted. The concentrations were determined using a Thermo Scientific (United States)-manufactured BCA protein kit. By using Western blotting, Hua et al. [30] analyzed tBid, Bax, Bcl-2, and caspase-3 expression patterns. Briefly, equal amounts of protein (25 μg) from each sample were loaded into gels and separated by SDS-PAGE (12% w/v polyacrylamide gel with a 5% w/v stacking gel). The gels were then electroblotted onto a polyvinylidene fluoride transfer membrane (Millipore, Bedford, Massachusetts). Immunoblots were probed with primary antibodies against Bax, Bcl-2, caspase-3, and tBid (sc-7480, sc-492, and sc-7272 from SANTA CRUZ BIOTECHNOLOGY, INC; ab10640 from Abcam; United States), and β -actin, a housekeeping protein, was used as a control and detected with monoclonal anti- β -actin (sc-47778 from SANTA CRUZ BIOTECHNOLOGY) and anti-mouse IgG-peroxidase conjugate (A2304, Sigma-Aldrich) as primary and secondary antibodies, respectively. 3,3'-diaminobenzidine (DAB; Sigma-Aldrich, D-7304) and H_2O_2 were used as substrates. The resulting images were captured using a ChemiDoc XRS imaging system (Bio-Rad, USA) in the presence of an enhanced chemiluminescence (ECL) solution.

4.6. Apoptosis assay via flow cytometry

For this experiment, 2×10^5 cells/mL MCF-7 cells were evenly distributed into individual wells of 6-well plates. The cells were then treated with 30% of the IC_{50} concentrations of DOX (0.36 μM), Zm-093 (22 μM), and a combination of both compounds (DOX + Zm-093: 0.36 + 22 μM) for 24 hours. A fluorescein isothiocyanate (FITC) Annexin V Apoptosis Detection Kit (Elabscience, USA) was used to analyze cell death [31]. In the subsequent procedure, the cells were collected and subjected to two rounds of washing with PBS. After 3 μL of FITC Annexin V and 3 μL of propidium iodide (PI; 1 mg/mL) were added to the suspensions, the mixtures were thoroughly combined and subjected to a 20 min incubation period at room temperature under light-restricted conditions. A Becton-Dickinson FACSCalibur™ flow cytometer was used to assess apoptosis, and FlowJo software version 7.6.1 was used to process the data (FlowJo LLC, Ashland, OR).

4.7. TUNEL Assay

Cell apoptosis rates were measured in various treatment groups using the TUNEL test. The cells were inoculated into 6-well plates at a concentration of 2×10^5 cells/mL and incubated overnight [32]. The cells were incubated at concentrations of 0.36 μ M and 14.5 μ M for 24 h for DOX alone or in combination with Zm-093, respectively. A TUNEL Assay Kit (Enhanced FITC, Elabscience: E-CK-A334) was used to determine the proportion of apoptotic cells. This procedure was performed following the manufacturer's guidelines. To summarize, the slides were subjected to two rounds of xylene administration, each lasting 5 min, followed by immersion in 100% and 95% ethanol for 3 min. The slides were subjected to two rounds of washing, each lasting 2 min, utilizing a solution composed of Tween 20-PBS. To inhibit peroxidase activity, the slides were incubated for 10 min in a PBS solution containing 3% hydrogen peroxide (H_2O_2). Subsequently, the slides were washed three times with a Tween 20-PBS solution for 2 min per wash. Next, the slides were incubated for 40 min in Buffer Reaction Terminal Deoxynucleotidyl Transferase (TdT), followed by a 1 h incubation in Mixture Reaction TdT at 37°C. Subsequently, the slides were washed with buffer wash stop for 4 min and then subjected to three washes with Tween 20-PBS, each lasting 2 min. The slides were incubated with HRP-streptavidin for 20 min at ambient temperature, followed by three washes with Tween 20-PBS for 2 min each. Subsequently, the slides were subjected to a 1 min incubation period with DAB, after which the slides were further washed with water. The slides were immersed in a hematoxylin solution for 30 seconds. Following this step, the slides were rinsed with water and dehydrated in 95% and 100% ethanol for 3 min. After they were double immersed in xylene for 5 min each, the cells were mounted. Fluorescence microscopy (Olympus BX50; Japan) was used to obtain the images.

4.8. Statistical analysis

The data for these experiments were analyzed via SPSS software (version 23.0) and GraphPad Prism (version 8.0). All the numerical data are presented as the means \pm standard deviations (SD), and all the experiments were repeated three times. Significant differences between groups were analyzed by one-way analysis of variance (ANOVA) and post hoc Duncan's test for multiple comparisons. Additionally, the one-sample t test was used to assess the significance of the observed differences between various groups. The significance level was set at $P < 0.00001$.

5. Conclusions

The current investigation showed that all CI acquired were less than one, suggesting a synergistic correlation between DOX and Zm-093 in terms of their anticancer efficacy against MCF-7 cells. The results of the Western blot analysis demonstrated the synergistic effect of DOX and Zm-093 on the protein expression levels of Bcl-2, tBid, and caspase-3, as well as the Bax/Bcl-2 ratio. Furthermore, the concurrent administration of these two compounds resulted in the initiation of programmed cell death (apoptosis) in MCF-7 cells via the intrinsic mechanism of apoptosis. These findings were subsequently validated through flow cytometry and TUNEL staining. The administration of substantial doses of DOX and Zm-093 individually is also limited by cytotoxicity and solubility issues. By administering DOX and Zm-093 together, these undesirable effects could be minimized, and drug resistance could be mitigated.

Supplementary Materials:

Acknowledgments: The authors are grateful to the University of Guilan for its support in conducting this study.

Policy and ethics: This article has been submitted in compliance with institutional policies regarding the ethical and humane treatment of experimental subjects, and the authors are willing to share the original data and materials if requested.

Author Contributions statement: **Shabnam Pedarpour:** Performing the experiments, Writing –original draft, Statistical Analysis. **Sevda Zarei:** Writing–original draft, Statistical Analysis. **Zeinab Mahmoodi:** Performing the experiments. **Hossein Ghafouri:** Conceptualization, Supervision, Methodology, Writing – review & editing.

Declaration of competing interest: The authors declare that there are no conflicts of interest or personal relationships that could influence their work.

References

1. R.L. Siegel, K.D. Miller, H.E. Fuchs, A. Jemal, Cancer statistics, 2021, *Ca Cancer J Clin.* 71 (2021) 7–33.
2. H. Sung, J. Ferlay, R.L. Siegel, M. Laversanne, I. Soerjomataram, A. Jemal, F. Bray, Global Cancer Statistics 2020: GLOBOCAN Estimates of Incidence and Mortality Worldwide for 36 Cancers in 185 Countries, *CA. Cancer J. Clin.* 71 (2021) 209–249. <https://doi.org/10.3322/caac.21660>.
3. A.G. Waks, E.P. Winer, Breast Cancer Treatment: A Review, *JAMA - J. Am. Med. Assoc.* 321 (2019) 288–300. <https://doi.org/10.1001/jama.2018.19323>.
4. K. Ghatreh Samani, E. Farrokhi, A. Tabatabaee, N. Jalilian, M. Jafari, Synergistic effects of lauryl gallate and tamoxifen on human breast cancer cell, *Iran. J. Public Health.* 49 (2020) 1324–1329. <https://doi.org/10.18502/ijph.v49i7.3586>.
5. M. Piralí, M. Taheri, S. Zarei, M. Majidi, H. Ghafouri, Artesunate, as a HSP70 ATPase activity inhibitor, induces apoptosis in breast cancer cells, *Int. J. Biol. Macromol.* 164 (2020) 3369–3375. <https://doi.org/10.1016/j.ijbiomac.2020.08.198>.
6. Z. Jahangirzadeh, H. Ghafouri, R.H. Sajedi, R. Sariri, S. Hossienkhani, Rapid and simple screening of the apoptotic compounds based on Hsp70 inhibition using luciferase as an intracellular reporter, *Anal. Bioanal. Chem.* 412 (2020) 149–158. <https://doi.org/10.1007/s00216-019-02220-3>.
7. C.M. Pfeffer, A.T.K. Singh, Apoptosis: A target for anticancer therapy, *Int. J. Mol. Sci.* 19 (2018) 448. <https://doi.org/10.3390/ijms19020448>.
8. A. Emami, H. Ghafouri, R. Sariri, Polyphyllin D-loaded solid lipid nanoparticles for breast cancer: Synthesis, characterization, in vitro, and in vivo studies, *Int. J. Pharm.* 639 (2023) 122976. <https://doi.org/10.1016/j.ijpharm.2023.122976>.
9. B. Alberts, A. Johnson, J. Lewis, D. Morgan, M. Raff, K. Roberts, P. Walter, *Molecular Biology of the Cell*, Garland science, 2017. <https://doi.org/10.1201/9781315735368>.
10. M. Namjoo, H. Ghafouri, E. Assareh, A.R. Aref, E. Mostafavi, A. Hamrahi Mohsen, S. Balalaie, S. Broussy, S.M. Asghari, A VEGFB-Based Peptidomimetic Inhibits VEGFR2-Mediated PI3K/Akt/mTOR and PLC γ /ERK Signaling and Elicits Apoptotic, Antiangiogenic, and Antitumor Activities, *Pharmaceuticals.* 16 (2023) 906. <https://doi.org/10.3390/ph16060906>.
11. R. Jan, G. e. S. Chaudhry, Understanding apoptosis and apoptotic pathways targeted cancer therapeutics, *Adv. Pharm. Bull.* 9 (2019) 205–218. <https://doi.org/10.15171/apb.2019.024>.
12. F. Hasanzadeh, H. Ghafouri, S. Ahmadi, S. Zarei, M.R. Aghamaali, A. Mohammadi, Inhibition of NF- κ B Expression in LPS-Induced RAW264.7 Macrophage Cells by a Thiazolidinone Derivative (TZDOCH 2 CH 3), *Avicenna J. Med. Biochem.* 9 (2021) 48–53. <https://doi.org/10.34172/ajmb.2021.09>.
13. Z. Xu, S.J. Zhao, Y. Liu, 1,2,3-Triazole-containing hybrids as potential anticancer agents: Current developments, action mechanisms and structure-activity relationships, *Eur. J. Med. Chem.* 183 (2019) 111700. <https://doi.org/10.1016/j.ejmech.2019.111700>.
14. X. Wang, H. Zhang, X. Chen, Drug resistance and combating drug resistance in cancer, *Cancer Drug Resist.* 2 (2019) 141–160. <https://doi.org/10.20517/cdr.2019.10>.
15. Y. Wan, G. Fang, H. Chen, X. Deng, Z. Tang, Sulfonamide derivatives as potential anti-cancer agents and their SARs elucidation, *Eur. J. Med. Chem.* 226 (2021) 113837. <https://doi.org/10.1016/j.ejmech.2021.113837>.
16. J.L. Robertson, M.M. Jones, E. Olguin, B. Alberts, *Bioassays with arthropods*, third edition, CRC press, 2017. <https://doi.org/10.1201/9781315373775>.
17. M. González-Álvarez, G. Alzuet, J. Borrás, L.D.C. Agudo, S. García-Granda, J.M. Montejo-Bernardo, Comparison of protective effects against reactive oxygen species of mononuclear and dinuclear Cu(II) Complexes with N-substituted benzothiazolesulfonamides, *Inorg. Chem.* 44 (2005) 9424–9433. <https://doi.org/10.1021/ic050110c>.
18. Z.H. Chohan, H.A. Shad, C.T. Supuran, Synthesis, characterization and biological studies of sulfonamide Schiff's bases and some of their metal derivatives, *J. Enzyme Inhib. Med. Chem.* 27 (2012) 58–68. <https://doi.org/10.3109/14756366.2011.574623>.
19. M. Salehi, F. Ghasemi, M. Kubicki, A. Asadi, M. Behzad, M.H. Ghasemi, A. Gholizadeh, Synthesis, characterization, structural study and antibacterial activity of the Schiff bases derived from sulfanilamides and related copper(II) complexes, *Inorganica Chim. Acta.* 453 (2016) 238–246. <https://doi.org/10.1016/j.ica.2016.07.028>.
20. A. Cumaoglu, S. Dayan, A.O. Agkaya, Z. Ozkul, N.K. Ozpazan, Synthesis and pro-apoptotic effects of new sulfonamide derivatives via activating p38/ERK phosphorylation in cancer cells, *J. Enzyme Inhib. Med. Chem.* 30 (2015) 413–419. <https://doi.org/10.3109/14756366.2014.940938>.

21. P.A.J. Speth, Q.G.C.M. van Hoesel, C. Haanen, Clinical Pharmacokinetics of Doxorubicin, *Clin. Pharmacokinet.* 15 (1988) 15–31. <https://doi.org/10.2165/00003088-198815010-00002>.
22. K. Chatterjee, J. Zhang, N. Honbo, J.S. Karliner, Doxorubicin cardiomyopathy, *Cardiology.* 115 (2010) 155–162. <https://doi.org/10.1159/000265166>.
23. G. Yang, J. Xing, B. Aikemu, J. Sun, M. Zheng, Kaempferol exhibits a synergistic effect with doxorubicin to inhibit proliferation, migration, and invasion of liver cancer, *Oncol. Rep.* 45 (2021) 1–10. <https://doi.org/10.3892/or.2021.7983>.
24. S. Tarazi, S. Ahmadi, N. Ostvar, H. Ghafouri, S. Sarikhan, Z. Mahmoodi, R. Sariri, Enhanced soluble expression of glutathione S-transferase Mu from *Rutilus kutum* by co-expression with Hsp70 and introducing a novel inhibitor for its activity, *Process Biochem.* 111 (2021) 261–266. <https://doi.org/10.1016/j.procbio.2021.10.003>.
25. V. Akbary Moghaddam, V. Kasmaeifar, Z. Mahmoodi, H. Ghafouri, O. Saberi, A. Mohammadi, A novel sulfamethoxazole derivative as an inhibitory agent against HSP70: A combination of computational with in vitro studies, *Int. J. Biol. Macromol.* 189 (2021) 194–205. <https://doi.org/10.1016/j.ijbiomac.2021.08.128>.
26. L. Jamalzadeh, H. Ghafoori, R. Sariri, H. Rabuti, J. Nasirzade, H. Hasani, M.R. Aghamaali, Cytotoxic Effects of Some Common Organic Solvents on MCF-7, RAW-264.7 and Human Umbilical Vein Endothelial Cells, *Avicenna J. Med. Biochem.* In press (2016). <https://doi.org/10.17795/ajmb-33453>.
27. S. Zarei, H. Ghafouri, L. Vahdatiraad, V.A. Moghaddam, T. Sohrabi, B. Heidari, Using heat shock protein (HSP) inducers as an approach to increase the viability of sterlet (*Pisces; Acipenseridae; Acipenser ruthenus*) cells against environmental diazinon toxicity, *J. Hazard. Mater.* 465 (2024) 133194. <https://doi.org/10.1016/j.jhazmat.2023.133194>.
28. N. Zhang, J.N. Fu, T.C. Chou, Synergistic combination of microtubule targeting anticancer fludellone with cytoprotective panaxytriol derived from panax ginseng against MX-1 cells in vitro: Experimental design and data analysis using the combination index method, *Am. J. Cancer Res.* 6 (2016) 97–104.
29. T.C. Chou, Theoretical basis, experimental design, and computerized simulation of synergism and antagonism in drug combination studies, *Pharmacol. Rev.* 58 (2006) 621–681. <https://doi.org/10.1124/pr.58.3.10>.
30. F. Hua, M.G. Cornejo, M.H. Cardone, C.L. Stokes, D.A. Lauffenburger, Effects of Bcl-2 levels on Fas signaling-induced caspase-3 activation: molecular genetic tests of computational model predictions, *J. Immunol.* 175 (2005) 985–995.
31. I. Lakshmanan, S. Batra, Protocol for Apoptosis Assay by Flow Cytometry Using Annexin V Staining Method, *Bio-Protocol.* 3 (2013) e374–e374. <https://doi.org/10.21769/bioprotoc.374>.
32. S.S. Singh, D.C. Mehedint, O.H. Ford, D.A. Jeyaraj, E.A. Pop, S.J. Maygarden, A. Ivanova, R. Chandrasekhar, G.E. Wilding, J.L. Mohler, Comparison of ACINUS, caspase-3, and TUNEL as apoptotic markers in determination of tumor growth rates of clinically localized prostate cancer using image analysis, *Prostate.* 69 (2009) 1603–1610. <https://doi.org/10.1002/pros.21019>.
33. M.P. Decatris, S. Sundar, K.J. O'Byrne, Platinum-based chemotherapy in metastatic breast cancer: Current status, *Cancer Treat. Rev.* 30 (2004) 53–81. [https://doi.org/10.1016/S0305-7372\(03\)00139-7](https://doi.org/10.1016/S0305-7372(03)00139-7).
34. A. Shafei, W. El-Bakly, A. Sobhy, O. Wagdy, A. Reda, O. Aboelenin, A. Marzouk, K. El Habak, R. Mostafa, M.A. Ali, M. Ellithy, A review on the efficacy and toxicity of different doxorubicin nanoparticles for targeted therapy in metastatic breast cancer, *Biomed. Pharmacother.* 95 (2017) 1209–1218. <https://doi.org/10.1016/j.biopha.2017.09.059>.
35. P.K. Singal, N. Iliskovic, Doxorubicin-induced cardiomyopathy, *N. Engl. J. Med.* 339 (1998) 900–905.
36. J.O. Tun, L.A. Salvador-Reyes, M.C. Velarde, N. Saito, K. Suwanborirux, G.P. Concepcion, Synergistic cytotoxicity of renieramycin M and doxorubicin in MCF-7 breast cancer cells, *Mar. Drugs.* 17 (2019) 536. <https://doi.org/10.3390/md17090536>.
37. M. Baravordah, H. Ghafouri, A. Mohammadi, S. Zarei, Design, Synthesis and Biological Evaluation of a Novel Sulfonamide Derivative as antiproliferative agents for Human Breast Cancer Cell line (MCF-7), *Modares J. Biotechnol.* 12 (2022) 91–102. <https://biot.modares.ac.ir/article-22-45276-en.html>.
38. R.P. Wurz, L. Liu, K. Yang, N. Nishimura, Y. Bo, L.H. Pettus, S. Caenepeel, D.J. Freeman, J.D. McCarter, E.L. Mullady, T.S. Miguel, L. Wang, N. Zhang, K.L. Andrews, D.A. Whittington, J. Jiang, R. Subramanian, P.E. Hughes, M.H. Norman, Synthesis and structure-activity relationships of dual PI3K/mTOR inhibitors based on a 4-amino-6-methyl-1,3,5-triazine sulfonamide scaffold, *Bioorganic Med. Chem. Lett.* 22 (2012) 5714–5720. <https://doi.org/10.1016/j.bmcl.2012.06.078>.
39. K. Greish, M. Fateel, S. Abdelghany, N. Rachel, H. Alimoradi, M. Bakhiet, A. Alsaie, Sildenafil citrate improves the delivery and anticancer activity of doxorubicin formulations in a mouse model of breast cancer, *J. Drug Target.* 26 (2018) 610–615. <https://doi.org/10.1080/1061186X.2017.1405427>.

40. K. Lin, Y. Rong, D. Chen, Z. Zhao, H. Bo, A. Qiao, X. Hao, J. Wang, Combination of Ruthenium Complex and Doxorubicin Synergistically Inhibits Cancer Cell Growth by Down-Regulating PI3K/AKT Signaling Pathway, *Front. Oncol.* 10 (2020) 141. <https://doi.org/10.3389/fonc.2020.00141>.
41. T.C. Chou, The mass-action law based algorithms for quantitative econo-green bio-research, *Integr. Biol.* 3 (2011) 548–559. <https://doi.org/10.1039/c0ib00130a>.
42. S. Elmore, Apoptosis: A Review of Programmed Cell Death, *Toxicol. Pathol.* 35 (2007) 495–516. <https://doi.org/10.1080/01926230701320337>.
43. A. Dezhpour, H. Ghafouri, S. Jafari, M. Nilkar, Effects of cold atmospheric-pressure plasma in combination with doxorubicin drug against breast cancer cells in vitro and in vivo, *Free Radic. Biol. Med.* 209 (2023) 202–210. <https://doi.org/10.1016/j.freeradbiomed.2023.10.405>.
44. J. Shi, J. Li, J. Li, R. Li, X. Wu, F. Gao, L. Zou, W.W.S. Mak, C. Fu, J. Zhang, G.P.H. Leung, Synergistic breast cancer suppression efficacy of doxorubicin by combination with glycyrrhetic acid as an angiogenesis inhibitor, *Phytomedicine.* 81 (2021) 153408. <https://doi.org/10.1016/j.phymed.2020.153408>.
45. J.S. Lee, E.K. Hong, *Hericium erinaceus* enhances doxorubicin-induced apoptosis in human hepatocellular carcinoma cells, *Cancer Lett.* 297 (2010) 144–154. <https://doi.org/10.1016/j.canlet.2010.05.006>.
46. K. Liu, S. Cang, Y. Ma, J.W. Chiao, Synergistic effect of paclitaxel and epigenetic agent phenethyl isothiocyanate on growth inhibition, cell cycle arrest and apoptosis in breast cancer cells, *Cancer Cell Int.* 13 (2013) 1–8. <https://doi.org/10.1186/1475-2867-13-10>.

Disclaimer/Publisher's Note: The statements, opinions and data contained in all publications are solely those of the individual author(s) and contributor(s) and not of MDPI and/or the editor(s). MDPI and/or the editor(s) disclaim responsibility for any injury to people or property resulting from any ideas, methods, instructions or products referred to in the content.